

Online characterization of planetary surfaces: PlanetServer, an open-source analysis and visualization tool.

R. Marco Figuera*, B. Pham Huu^a, A. P. Rossi^a, M. Minin^a, J. Flahaut^b, A. Halder^a

^a*Jacobs University Bremen, Campus Ring 1, 28759, Bremen, Germany*

^b*Institut de Recherche en Astrophysique et Planétologie, UMR 5277 du CNRS, Université Paul Sabatier, 31400 Toulouse, France.*

Abstract

The lack of open-source tools for hyperspectral data visualization and analysis creates a demand for new tools. In this paper we present the new PlanetServer, a set of tools comprising a web Geographic Information System (GIS) and a recently developed Python Application Programming Interface (API) capable of visualizing and analyzing a wide variety of hyperspectral data from different planetary bodies. Current WebGIS open-source tools are evaluated in order to give an overview and contextualize how PlanetServer can help in this matters. The web client is thoroughly described as well as the datasets available in PlanetServer. Also, the Python API is described and exposed the reason of its development. Two different examples of mineral characterization of different hydrosilicates such as chlorites, prehnites and kaolinites in the Nili Fossae area on Mars are presented. As the obtained results show positive outcome in hyperspectral analysis and visualization compared to previous literature, we suggest using the PlanetServer approach for such investigations.

Keywords: Mars, CRISM, open-source, WebGIS

1. Introduction

1.1. Scientific Background

The mineral characterization of planetary surfaces bears great importance for space exploration. Several studies have targeted a variety of minerals on Mars' surface based on imaging spectrometer data (Murchie et al. (2009), Bibring et al. (2006), Liu et al. (2016), Cuadros and Michalski (2013), Brown et al. (2010), Poulet et al. (2005) and Ehlmann et al. (2009)). Most of those studies have been carried out using VNIR spectroscopic data from the Observatoire

*Corresponding author

Email address: r.marcofiguera@jacobs-university.de (R. Marco Figuera)

pour la Minéralogie, l'Eau, les Glaces et l'Activité (OMEGA, Mars Express) (Bibring et al. (2004)) and Compact Reconnaissance Imaging Spectrometer for Mars (CRISM, Mars Reconnaissance Orbiter)(Murchie et al. (2007)) imagery combined with different Digital Terrain Models (DTMs) of the areas. Accessing hyperspectral data stored in different planetary science data archives is a straightforward process. Nevertheless, analysis tools are often costly and methods tend to be hard to implement. Usually, the software used to process as well as to analyze data is the ENvironment for Visualizing Images (ENVI) package. Both OMEGA and CRISM experiment teams provided the science community with a set of IDL/ENVI routines (SOFT for OMEGA, CAT for CRISM) that allow basic processing steps. CAT for CRISM also includes the CRISM products described in Viviano-Beck et al. (2014) allowing to create RGB band math combinations. In this document we present the current status of PlanetServer an open-source and ready-to-use online tool providing access to visualization and analysis of Mars CRISM and Moon Mineralogy Mapper (M3) images using the Web Coverage Processing Service (WCPS) Open Geospatial Consortium (OGC) standard, with the possibility of supporting more experiment and target Solar System bodies.

1.2. State of the art in planetary web services

In the last years several planetary web services have been developed. Planetary web services cover a broad list of needs for the scientific community: from data exploration and retrieving to analysis and exploitation. Mars trek¹, a web visualization service provided by NASA, showcases different data collected by a variety of instruments at selected landing sites. In this case, the service is more an outreach tool rather than an analysis tool. The service also offers data from the Moon² (Day and Law (2016)) and Vesta³. The PDS geoscience node also provides the so called Orbital Data Explorer (ODE)⁴, a set of tools for visualization of Mars, Moon, Mercury and Venus data stored in PDS. The ODE Map search allows to focus on a Region of Interest (RoI) and select the datasets to download using point or polygon selection. A feature shared among the majority of visualization services is the selection of features by clicking or by a polygon and the change of cartographic projection.

The recently developed Multi-Temporal Database of Planetary Image Data (MUTED) (Erkeling et al. (2016)) is an online web service providing different spatial and temporal Martian datasets based on a polygon selection⁵. An asset of MUTED is the possibility to retrieve data based on temporal or spatial parameters of a selected RoI, thus making it very convenient and appropriate when multiple multi-temporal datasets exist. Another web service is i-mars⁶

¹<http://marstrek.jpl.nasa.gov>

²<http://moontrek.jpl.nasa.gov>

³<http://vestatrek.jpl.nasa.gov>

⁴<http://ode.rsl.wustl.edu>

⁵<http://muted.wvu.de/>

⁶<http://www.i-mars.eu/web-gis>

(van Gasselt et al. (2014)) providing online visualization of selected datasets.

While the above mentioned services focus on the visualization and data retrieval, different services exist that allow the user to process and analyze data online. The MARS Information System (MarsSI)⁷ (Lozac'h et al. (2015)), a web application developed at the Université Lyon 1, allows the user to select raw Martian data (HiRISE, CTX, CRISM, OMEGA, etc) and process them using built-in pipelines. The output is data that can be loaded into a GIS. While MarsSI allows selection and processing of data it does not visualize the final product in-situ neither allows to interactively analyze the data. In order to use MarsSI one needs to register by filling a form provided at their website, thus making the access to the tool cumbersome. The Planetary Surface Portal (PSUP)⁸ (Poulet et al., this special issue) combines in one platform the processing power of MarsSI together with the visualization tool MarsVisu. PSUP allows the user to analyze and visualize data from a wide variety of datasets within the same environment.

The old version of PlanetServer (Chiwome (2014) and Oosthoek et al. (2015)) developed within the EU FP7-INFRA project EarthServer was the predecessor and initial client of the actual PlanetServer. The old client provided visualization and analysis of CRISM data through a web portal using openlayers and self made tools. The visualization was presented as a 2D map and the analysis and selection tools were displayed on top of the main map. The architecture of the old PlanetServer was very similar to the actual client, using rasdaman as the database manager software and WCPS queries in order to access the data.

If we analyze the capabilities of the above mentioned web services, with the exception of the old PlanetServer, we quickly realize the lack of in-situ analysis tools and online output files visualization. With the new version of PlanetServer we aim to cover this gap in the current available web services by adding the possibility to analyze data in real-time and present the output results without leaving the web environment. This is possible by adopting the WCPS OGC standard discussed in detail in the following chapters.

After a description of the architecture, datasets and features of PlanetServer (section 2), we introduce the PlanetServer Python API (section 2.1.1). Afterwards, we demonstrate the tool reliability with some examples of analysis carried out with PlanetServer (section 2.4). Finally, discussions and ongoing work are presented.

2. PlanetServer

PlanetServer is the planetary service of the H2020 EC-funded project EarthServer-2 (Baumann et al. (2015)) aiming at access and exploitation of Big Earth Science data. The project comprises various services related to specific domains (Earth Observation, Marine Remote Sensing and Climate Modeling). The planetary

⁷<https://emars.univ-lyon1.fr/MarsSI>

⁸<http://psup.ias.u-psud.fr>

section of the project is developed at Jacobs University Bremen and it focuses on the visualization and analysis of space mission data on solid planets and moons, using OGC standards on a web client based on the JavaScript version of NASA’s World Wind (Gaskins (2009)) and a Python API. PlanetServer is currently divided in two web clients containing Mars CRISM data and Moon Mineral Mapper (M3) (Pieters et al. (2009), Green et al. (2011)) data and a Python API capable of accessing and analyzing both datasets. The Python API will be further discussed in section 2.1.1.

2.1. Architecture

As Figure 1 highlights, the service architecture has two components: the server and the client side. In the server side the download, preprocessing and storage of the data takes place.

M3 and CRISM datasets are publicly available in the Planetary Data Service (PDS) archives (McMahon (1996)), after limited embargo periods. Therefore the retrieval of planetary data from different missions and instruments is a straightforward process. The data are downloaded using a set of dedicated scripts that search for the entire CRISM and M3 catalogs in the PDS archive. Data reduction and processing historically relies largely on users, although recent initiatives provide server side pre-processing (Hare et al. (2014)). The data is subsequently processed in our servers in order to apply the necessary atmospheric corrections and map projections. A more detailed explanation of the data download and preprocessing is explained in section 2.3.1. Finally, data are stored using the Array DataBase Management System (DBMS) Raster Data Manager (Rasdaman), capable of storage and retrieval of multidimensional data (Baumann et al. (1998)). Rasdaman is an Array DBMS offering features such as query languages, query optimization and parallelization on n-D arrays. The Rasdaman data model consists of n-D arrays with individually fixed or variable boundaries. The query language, rasql, is an ISO SQL extended language allowing declarative array selection and processing with multidimensional operators. The array is partitioned (tiled) and stored along with the processing engine, thus reducing the query response time. OGC standards such as the WCPS (Baumann (2010)), are implemented in the PetaScope component (Aiordchioaie and Baumann (2010)), a set of geospatial and geometry libraries, data access libraries and relational database access components.

In the client side, two different methods are available for data visualization and analysis. Using the web client, the data is visualized using NASA’s Web World Wind allowing access through a web interface. NASA Web World Wind is a general-purpose 3D/4D client used as a virtual globe to interactively analyze and visualize data. As Web World Wind is completely open-source, one can easily extend its functionality and Application Programming Interface (API) to fit in the project purposes. The API has been developed for HTML5 and JavaScript and uses WebGL as a rendering engine. PlanetServer extensively uses OGC standards (WMS and WCPS) in order to retrieve, visualize and compute data. The web client contains two main features, the RGB combinations and Spectral analysis tools. Using the Python API or Jupyter notebooks the user

has access to the same features as in the web client. Data visualization and analysis using PlanetServer’s Python API is further discussed in section 2.1.1.

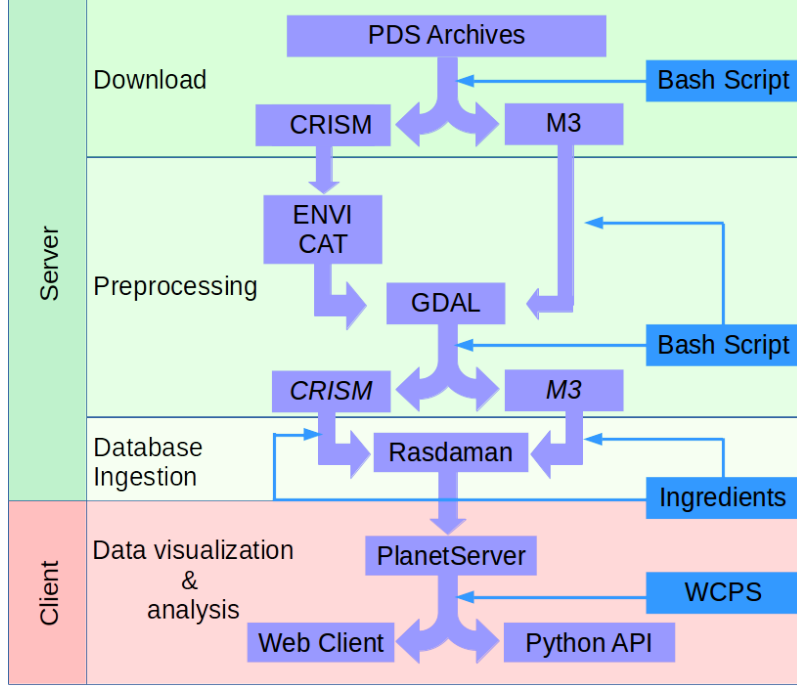


Figure 1: This figure shows the PlanetServer pipeline covering all the process. The data is downloaded from PDS archive, processed using ENVI CAT and GDAL for CRISM, and only GDAL for M3. Data are ingested into Rasdaman. PlanetServer’s data can be accessed using the web client or the Python API.

2.1.1. Python API

As Python is gaining a remarkable popularity among the planetary science and astronomy community, we developed the PlanetServer Python API. The tool is available as a Python package that can be integrated in existing python pipelines as well as a Jupyter notebook, capable of running in a browser. The API integrates the features available in the web client: RGB combinations and spectral analysis tools.

In order to create the CRISM products, we created a dictionary in JSON format where a set of parameters are given:

Listing 1: Declaration of CRISM products in JSON format.

```

1 summary_products = {
2   "BD1300" : [f1, ["R1320", "R1080", "R1750"]],
3   "BD1400" : [f1, ["R1395", "R1330", "R1467"]],
4   "BD1435" : [f1, ["R1435", "R1370", "R1470"]],
5   "BD1500-2" : [f1, ["R1525", "R1367", "R1808"]],
6   ...

```

7 }

The first parameter (BD1300) is the name of the CRISM product. This name will be used when creating the RGB combination. The second parameter (f1) is the family type. CRISM products have been grouped based on their similarities⁹ thus speeding the definition process. The last parameters are the wavelengths that compose the product (R_c being the central wavelength, R_s the shorter wavelength and R_L the longer wavelength, given in this order).

As illustrated in Figure2, the Python API has been constructed such that a user only needs to give five input arguments to the API: The coverage ID, the name of three CRISM summary products that are stored in each channel (Red, Green and Blue) and the name of a table containing the relation between the band names and the corresponding wavelengths. The table has been created using Astropy and extracting the metadata attached to any CRISM image. The script to create tables for new datasets is provided in the package. The API combines the 3 summary products into a WCPS query giving an image as output. The spectral analysis tool will be activated by clicking a point in the image. All the plots and images can be downloaded for further editing.

⁹The family definition is available on the Jupyter notebook inside PlanetServers' GitHub repository: https://github.com/planetserver/PS_Python_API

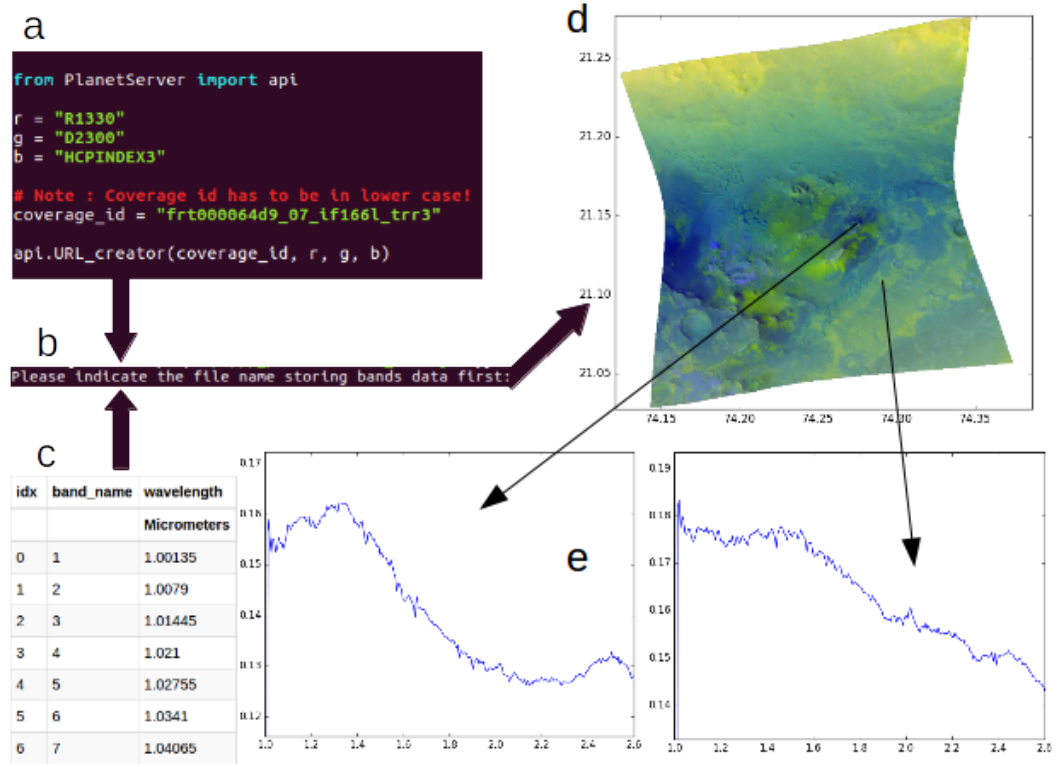


Figure 2: PlanetServer Python API workflow. a) The user inputs the three CRISM summary products in the corresponding RGB channels (R:LCPINDEX2, G:D2200 and B:HCPINDEX3) and the coverage ID. b) A Flexible Image Transport System (FITS) table (provided in the package) with the relation between band names and wavelengths (c) needs to be called in order to create correct WCPS queries. d) The API outputs an image containing the RGB combination. e) By clicking a location in the image (e.g: 21.19°N, 74.24°E), the API will show the spectral profile.

2.2. Features

PlanetServer's web client has been developed in a non-invasive and minimalist way. The client is divided in 4 areas (Figure 3) containing the Globe and different docks.

- Navigation bar: The navigation bar (located in the upper part) contains links to the service description website and the project description website as well as the Moon and Mars icon to navigate between planets.
- Main dock: Located in the left part of the client, the main dock contains: projections, available base maps, search engine (by location, name and coordinates) and the RGB combination tool (this feature is further discussed in section 2.2.1).

- Secondary dock: Located in the right part of the client, the secondary dock contains 3 sub-docks: The spectral plot and spectral ratio dock (where the spectral analysis tool (discussed in section 2.2.2) is used), and the information dock (which contains information about the client, a contact form as well as a tour, guiding the user through the client showing all the functionalities).
- Globe: In the central part of the client the Globe is shown. Depending on the client, either the Moon or Mars will be loaded.
- Coordinate and Elevation: Located in the bottom right part of the client are the coordinates, elevation and eye altitude information at the current position.

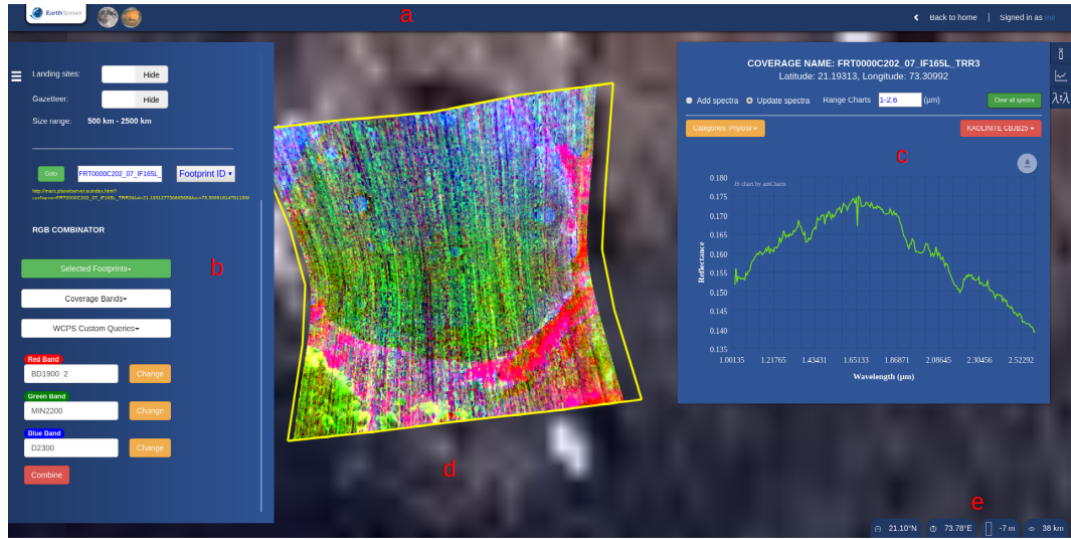


Figure 3: PlanetServer web client outlook. a) The navigation bar is shown in the upper part of the client. It allows the user to navigate through the different available planetary bodies. b) The main dock, located in the left part, contains the layers, search and RGB combination tool. c) shows the plotting dock where all the spectral analysis is carried out. d) The main globe accommodates the georeferenced analyzed images. e) The latitude, longitude, altitude as well as height information is shown.

PlanetServer uses extensively OGC standards in order to retrieve graphic information. WMS is an OGC standard allowing the user to retrieve images hosted on a server. In PlanetServer, WMS is used to retrieve base maps as well as deploy the DTMs. An innovative feature of PlanetServer is the use of WCPS, allowing the user to retrieve images by setting different parameters such as area, time, bands, etc. The main difference to other OGC standards is that the WCPS retrieved image is not static and can be changed by updating the parameters.

2.2.1. RGB combination tool

The RGB combination tool allows the user to create different RGB combinations by selecting single or multiple images and a set of bands or CRISM products to be combined in each channel. As multiple selection is possible, the same RGB combination can be processed in several images at once. Also, when images overlap the user can select the desired image and lock it, thus targeting the desired image.

One of the key features of PlanetServer is the possibility to retrieve different CRISM summary products allowing to pursue better enhance and better visualize different materials in an image. We have translated the CRISM summary products (Viviano-Beck et al. (2014)) to WCPS and allow access through the web client and the Python API. A list of 44 summary products are currently available (Table 1). The tool combines three CRISM products in each RGB channel and creates a WCPS query to compute the combination. The output of this query is a TIFF image which is temporary downloaded into our servers. In order to enhance and better visualize the image we set a fixed stretching values. The mean value (μ) of each channel as well as the standard deviation (σ) is calculated using the Geospatial Data Abstraction Library (GDAL) and the image is re-stretched using as minimum value $\mu - 1.5 * \sigma$ and maximum value $\mu + 1.5 * \sigma$. The image is then send back to PlanetServer in PNG format to be displayed in the globe. Currently, this stretching values are fixed and shared among all the RGB combinations. Ongoing work includes the possibility to dynamically change the stretching values according to the user needs. At present, the CRISM RGB combinations created with PlanetServer are not considering any thresholds and all data is taken into account. Ongoing work includes setting a threshold greater than 0 in order to avoid the background noise. As stated by Carter et al. (2013b) several artifacts can occur in the RGB combinations when specific corrections are not applied to the original data. We are currently studying the possibility of adding such corrections in order to prevent such artifacts.

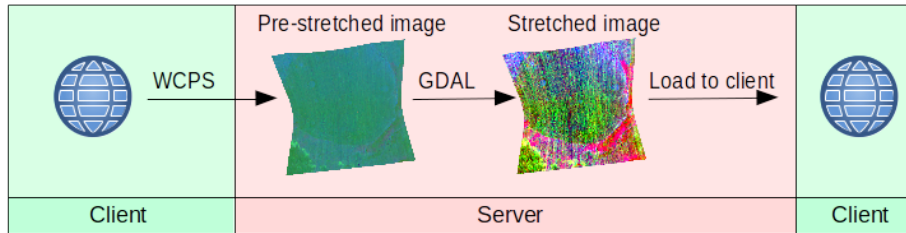


Figure 4: Workflow of the RGB combination. The tool combines the selected CRISM products and creates a WCPS query. The query computes an image where the minimum and maximum values cover the entire histogram. GDAL is run on the image to extract the mean value and standard deviation of each band. After applying the new stretching values the image is then send to the client or Python API.

Name	Parameter	Equation	Notes
BD1300	1.3 μm absorption associated with Fe^{2+}	$1 - \left(\frac{R1320}{a \cdot R1080 + b \cdot R1750} \right)$	Plagioclase with Fe^{2+} substitution
BD1400	1.4 μm H_2O and OH band depth	$1 - \left(\frac{R1395}{a \cdot R1330 + b \cdot R1467} \right)$	Hydrated or hydroxylated minerals
BD1435	1.435 μm CO_2 ice band depth	$1 - \left(\frac{R1435}{a \cdot R1370 + b \cdot R1470} \right)$	CO_2 ice, some hydrated minerals
BD1500_2	1.5 μm H_2O ice band depth	$1 - \left(\frac{R1525}{a \cdot R1367 + b \cdot R1808} \right)$	H_2O ice on surface or in atmosphere
BD1750_2	1.7 μm H_2O band depth	$1 - \left(\frac{R1750}{a \cdot R1690 + b \cdot R1815} \right)$	Gypsum, Alunite
BD2100_2	2.1 μm shifted H_2O band depth	$1 - \left(\frac{R2132}{a \cdot R1930 + b \cdot R2250} \right)$	H_2O monohydrated sulfates
BD2165	2.165 μm Al–OH band depth	$1 - \left(\frac{R2165}{a \cdot R2120 + b \cdot R2230} \right)$	Pyrophyllite, kaolinites
BD2190	2.190 μm Al–OH band depth	$1 - \left(\frac{R2185}{a \cdot R2120 + b \cdot R2250} \right)$	Beidellite, Allophane, Imogolite
BD2210_2	2.215 μm Al–OH band depth	$1 - \left(\frac{R2210}{a \cdot R2165 + b \cdot R2250} \right)$	Al–OH minerals
BD2230	2.23 μm band depth	$1 - \left(\frac{R2235}{a \cdot R2210 + b \cdot R2252} \right)$	Hydroxylated ferric sulfate
BD2250	2.25 μm broad Al–OH and Si–OH band depth	$1 - \left(\frac{R2245}{a \cdot R2120 + b \cdot R2340} \right)$	Opeal and other Al–OH minerals
BD2265	2.265 μm band depth	$1 - \left(\frac{R2265}{a \cdot R2210 + b \cdot R2340} \right)$	Jarosite, Gibbsite, Acid-leached nontronite

Name	Parameter	Equation	Notes
BD2290	2.3 μm Mg, Fe–OH band depth and 2.292 μm CO ₂ ice band depth	$1 - \left(\frac{R2290}{a \cdot R2250 + b \cdot R2350} \right)$	Mg, Fe–OH minerals and CO ₂ ice
BD2355	2.53 μm band depth	$1 - \left(\frac{R2355}{a \cdot R2300 + b \cdot R2450} \right)$	Chlorite, Prehnite, Pumpellyite
BD2500_2	Mg carbonate overtone band depth	$1 - \left(\frac{R2480}{a \cdot R2364 + b \cdot R2570} \right)$	Mg carbonates
BD3100	3.1 μm H ₂ O ice band depth	$1 - \left(\frac{R3120}{a \cdot R3000 + b \cdot R3250} \right)$	H ₂ O ice
BD3200	3.2 μm CO ₂ ice band depth	$1 - \left(\frac{R3320}{a \cdot R3250 + b \cdot R3390} \right)$	CO ₂ ice
BD3400_2	3.4 μm carbonate band depth	$1 - \left(\frac{R3420}{a \cdot R3250 + b \cdot R3630} \right)$	Carbonates
BD2600	2.6 μm H ₂ O band depth	$1 - \left(\frac{R2600}{a \cdot R2530 + b \cdot R2630} \right)$	H ₂ O vapor
MIN2200	2.16 μm Si–OH band depth and 2.21 μm H ⁺ bounds Si–OH band depth	$minimum \left[\left(1 - \left(\frac{R2165}{a \cdot R2120 + b \cdot R2350} \right) \right), \left(1 - \left(\frac{R2210}{a \cdot R2120 + b \cdot R2350} \right) \right) \right]$	Kaolinites
MIN2250	2.21 μm Si–OH band depth and 2.26 μm H ⁺ bounds Si–OH band depth	$minimum \left[\left(1 - \left(\frac{R2210}{a \cdot R2165 + b \cdot R2350} \right) \right), \left(1 - \left(\frac{R2265}{a \cdot R2165 + b \cdot R2350} \right) \right) \right]$	Opals

Name	Parameter	Equation	Notes
MIN2295_2480	Mg carbonate overtone band depth and metalOH band	$minimum \left[\left(1 - \left(\frac{R2295}{a \cdot R2165 + b \cdot R2364} \right) \right), \left(1 - \left(\frac{R2480}{a \cdot R2364 + b \cdot R2570} \right) \right) \right]$	Mg carbonates; both overtones must be present
MIN2345_2537	Ca/Fe carbonate overtone band depth and metalOH band	$minimum \left[\left(1 - \left(\frac{R2345}{a \cdot R2250 + b \cdot R2430} \right) \right), \left(1 - \left(\frac{R2537}{a \cdot R2430 + b \cdot R2602} \right) \right) \right]$	Ca/Fe carbonates; both overtones must be present
BD1900_2	1.9 μm H ₂ O band depth	$0.5 \cdot \left(1 - \left(\frac{R1930}{a \cdot R1850 + b \cdot R2067} \right) \right) + 0.5 \cdot \left(1 - \left(\frac{R1985}{a \cdot R1850 + b \cdot R2067} \right) \right)$	Bound molecular H ₂ O except monohydrated sulfates
R1330	IR albedo	$R1330$	IR albedo (ices > dust > unaltered mafics)
R1080	1.08 μm reflectance	$R1080$	Component of the false color RGB combination
R1506	1.51 μm reflectance	$R1506$	Component of the false color RGB combination
R2529	2.53 μm reflectance	$R2529$	Component of the visible to infrared false color RGB combination
R3920	2.53 μm reflectance	$R3920$	Component used in the ice detection RGB combination
IRR2	IR ratio 2	$\frac{R2530}{R2210}$	Aphelion ice clouds versus seasonal or dust
IRR3	IR ratio 3	$\frac{R3500}{R3390}$	Aphelion ice clouds (higher values) versus seasonal or dust

Name	Parameter	Equation	Notes
BD3000	3 μm H ₂ O band depth	$1 - \left(\frac{R3000}{R2530 \cdot \left(\frac{R2530}{R2210} \right)} \right)$	Bound H ₂ O (accounts for spectral slope)
SINDEX2	Inverse lever rule to detect convexity at 2.29 μm due to 2.1 μm and 2.4 μm absorptions	$1 - \left(\frac{a \cdot R2120 + b \cdot R2400}{R2290} \right)$	Hydrated sulfates (mono and poly hydrated sulfates) will be strongly > 0
CINDEX2	Inverse lever rule to detect convexity at 3.6 μm due to 3.4 μm and 3.9 μm absorptions	$1 - \left(\frac{a \cdot R3450 + b \cdot R3875}{R3610} \right)$	Carbonates will be > background values > 0
ISLOPE1	spectral slope 1	$\frac{R1815 - R2530}{W2530 - W1815}$	Ferric coating on dark rocks
ICER1.2	CO ₂ and H ₂ O ice band depth	$1 - \left(\frac{1 - BD1435}{1 - BD1500_2} \right)$	CO ₂ and H ₂ O ice mixtures; > 1 for more CO ₂ and > 1 for more H ₂ O
D2200	2.2 μm dropoff	$1 - \left(\frac{\frac{R2210}{RC2210} + \frac{R2230}{RC2230}}{2 \cdot \frac{R2165}{RC2165}} \right)^{10}$	Al–OH minerals
D2300	2.3 μm dropoff	$1 - \left(\frac{\frac{R2290}{RC2290} + \frac{R2320}{RC2320} + \frac{R2330}{RC2330}}{\frac{R2120}{RC2120} + \frac{R2170}{RC2170} + \frac{R2210}{RC2210}} \right)^{11}$	Hydroxylated Fe, Mg silicates strongly > 0
BD1900r2	1.9 μm H ₂ O band depth	$1 - \left(\frac{\frac{R1908}{RC1908} + \frac{R1914}{RC1914} + \frac{R1921}{RC1921} + \frac{R1928}{RC1928} + \frac{R1934}{RC1934} + \frac{R1941}{RC1941}}{\frac{R1862}{RC1862} + \frac{R1869}{RC1869} + \frac{R1875}{RC1875} + \frac{R2112}{RC2112} + \frac{R2120}{RC2120} + \frac{R2126}{RC2126}} \right)$	H ₂ O

¹⁰Slope for RC##### anchored at R1815 and R2430

¹¹Slope for RC##### anchored at R1815 and R2530

Name	Parameter	Equation	Notes
LCPINDEX2	Detect broad absorption centered at 1.8 μm	$RB1690 \cdot 0.20 + RB1750 \cdot 0.20 + RB1810 \cdot 0.30 + RB1870 \cdot 0.20$ ¹²	Pyroxene
HCPINDEX2	Detect broad absorption centered at 2.12 μm	$RB2120 \cdot 0.10 + RB2140 \cdot 0.10 + RB2230 \cdot 0.15 + RB2250 \cdot 0.30 + RB2430 \cdot 0.20 + RB2460 \cdot 0.15$ ¹³	Pyroxene
OLINDEX3	Detect broad absorption centered at 1 μm	$RB1080 \cdot 0.03 + RB1152 \cdot 0.03 + RB1210 \cdot 0.03 + RB1250 \cdot 0.03 + RB1263 \cdot 0.07 + RB1276 \cdot 0.07 + RB1330 \cdot 0.12 + RB1368 \cdot 0.12 + RB1395 \cdot 0.14 + RB1427 \cdot 0.18 + RB1470 \cdot 0.18$ ¹⁴	Olivines

Table 1: List of currently available CRISM products in Planet-Server. The table has been adapted from Viviano-Beck et al. (2014). Ongoing work will include the totality of the CRISM products in Viviano-Beck et al. (2014).

¹²Slope for RC##### anchored at R1560 and R2450

¹³Slope for RC##### anchored at R1690 and R2530

¹⁴Slope for RC##### anchored at R1750 and R2400

The a and b parameters in Table 1 are weighted parameters used to accurately represent the band depth of asymmetric absorption features when λ_C (center wavelength) is not centered between λ_S (short wavelength) and λ_L (long wavelength). They are calculated as follows:

$$b = \frac{\lambda_C - \lambda_S}{\lambda_L - \lambda_S} \quad (1)$$

$$a = 1 - b \quad (2)$$

2.2.2. Spectral Analysis tool

Spectra can be easily analyzed in PlanetServer. The Spectral Analysis tool is automatically triggered when clicking in a location of an image (in the web client the user needs to firstly open the designated dock). The tool collects the latitude and longitude of the clicked point, transform it into the same units as in the Coordinate Reference System (CRS) of the image and build a WCPS query to retrieve the spectral data. The server will produce a comma-separated file (CSV) that will be read by the tool. If the tool is used in the web client, the spectra will be shown in the plot dock and the user will be able to zoom in and out and load different laboratory spectra available in the PDS Geosciences Spectral Library¹⁵ or the USGS splib06a (Clark et al. (2007)) spectral library. The user can load one single spectra or collect multiple spectra. The multiselection of spectra is shown in different colors, so each spectra color corresponds to one location. The spectra collection is not reduced to one image allowing the user to collect data among different images. In case the tool is used in the Python API, a new window will be created each time a location is clicked. The API can currently analyze spectra in a single image at a time and spectral libraries are not yet automatically implemented although it is possible to add them manually within a few lines of code.

The tool is also used for spectral ratio calculations (currently available only in the web client). The spectral ratio is located in the ratio dock. Once the ratio dock is opened the user can select the denominator and numerator and click in the image to collect the spectra. A ratio is automatically computed and displayed. Both plots can be downloaded in different formats for further analysis outside PlanetServer.

2.3. Datasets

As Table 2 illustrates, PlanetServer contains three different types of data: Base maps, DTMs and hyperspectral images of Mars and the Moon. The Mars client includes a global Viking and colored Mars Orbiter Laser Altimeter (MOLA) shaded relief used as base map. The Moon client contains a global Lunar Reconnaissance Orbiter (LRO) WAC and a colored LOLA shaded relief base map. Base maps are served using the Web Mapping Service (WMS) OGC standard in both clients. While Viking and LRO WAC base maps endpoints are

¹⁵Available in: <http://speclib.rsl.wustl.edu>

located in our servers, MOLA and LOLA colored shaded relief base maps endpoints are located in the United States Geological Survey (USGS) servers. The main reason of having different endpoints is to test and prove interoperability between different endpoints of PlanetServer.

Mars' DTM is a global MOLA DTM served via WMS from GeoServer. The DTM deployed in the Moon client is a global LOLA DTM. Both DTMs are served from GeoServer as WorldWind only accepts BIL format to deploy the DTM and, at the moment, Rasdaman do not support such format. The original DTMs were transformed to BIL format using GDAL.

CRISM is an spectrometer on board NASA's Mars Reconnaissance Orbiter (MRO). CRISM Targeted Reduced Data Record (TRDR) covers visible to infrared spectra, from 0.362 to 3.92 μm . Each scene is split in two different images, one covering the range from 0.362 to 1 μm (S observations) and the other from 1.035 to 3.92 μm (L observations). CRISM TRDR images have been acquired with a detector temperature of $\sim 124^\circ K$. M3 is the image spectrometer on board Chandrayaan-1 Lunar Orbiter (CH-1), an Indian Space Research Organization Lunar orbiter. It covers the spectra from 0.43 to 3 μm . M3 images have been acquired with a detector temperature of $\sim 167^\circ K$. Both datasets are downloaded from the PDS archive and processed in our servers before ingesting them in Rasdaman (the process is discussed in section 2.3.1).

In Mars, we also serve the CRISM Multispectral Reduced Data Records (MRDR) dataset (currently in beta version). This dataset is a global tiled coverage of Mars build by mosaicking CRISM TRDR images. The dataset has been spectrally downsampled and separated in 3 different products: Spectral data images, false color images, and CRISM products images. In PlanetServer we currently serve only the CRISM products images. These cubes contain 43 bands with a computed CRISM product in each band. We use WCPS in order to select the bands in the RGB combination tool. Currently, we are testing the dataset behavior in PlanetServer.

In order to do spectral analysis in PlanetServer, the splib06a Clark et al. (2007) laboratory spectra library has been added to the service. The library contains a set of spectral profiles that can be loaded in the Spectral Analysis tool and compared to CRISM spectral profiles. In both clients, we added vectorial data showing the Moon's and Mars' Gazetteer and a list of landing sites.

2.3.1. Data processing

CRISM and M3 data have their particular processing pipeline before they can be ingested into rasdaman and be used in PlanetServer, and some rasdaman features need to be created in order to use non-Earth planetary science data. Although both pre-process pipelines have some similarities, each have special steps that need to be addressed. As stated in the introductory section both datasets are publicly available through the PDS archive, therefore obtaining the data is as simple as fetching the data from such archives.

In order to configure Rasdaman to work with the mentioned datasets, we created the CRS for the Moon and Mars and declared them in the Semantic Coordinate Reference System Resolver (SECORE)(Misev et al. (2012)), a server

Table 2: List of currently available datasets on PlanetServer.

Body	Dataset	Source	Level	N of cubes	Dataset size	Cube size	Pixel size	Retrieval
Mars	Base map	Viking	L4	1	12 GB	12 GB	233m/pix	WMS
	Base map ^a	MOLA	L4	1	–	–	463m/pix	WMS
	DTM	Mola global DTM	L4	1	2GB	2GB	463m/pix	WMS
	Hyperspectral Cubes	CRISM TRDR	L3	21659	9.6 TB	50 - 250 MB	20m/pix	WCPS
	CRISM products	CRISM MRDR	L4	99	21 GB	170 - 300 MB	232m/pix	WCPS
	Spectral laboratory data	splib06a	L4	1	–	–	–	WCPS
	Gazetteer	–	L4	1	–	–	–	WorldWind
	Landing sites	–	L4	1	–	–	–	WorldWind
	Moon							
	Base map	LRO WAC	L4	1	1.4GB	1.4GB	100m/pix	WMS
	Base map ^b	LRO WAC	L4	1	–	–	118m/pix	WMS
	DTM	LOLA	L4	1	8GB	8GB	118m/pix	WMS
	Hyperspectral cubes	M3	L2b	333	3.2 TB	500MB - 3GB	110m/pix	WCPS
	Gazetteer	–	L4	–	–	–	–	WorldWind
	Landing sites	–	L4	–	–	–	–	WorldWind

^aAs this base map is hosted at the USGS server we do not include the size of the dataset^bAs this base map is hosted at the USGS server we do not include the size of the dataset

which resolves CRS URLs into full CRS definitions represented in Geographic Markup Language (GML) 3.2.1. The CRS and SECORE will be further discussed in section 2.3.1

CRISM. We created a set of scripts to download CRISM V3 L2 data containing reflectance information, which search the entire CRISM catalog in the PDS archive. The script creates a file containing links to the available images. The file is later executed using `wget` in order to download the images. The search script can be used the first time to build the database and subsequently to update the existing database. In the later case it will check the existing list of images in PlanetServer and compare to the list in the PDS archive. In case new data are available, the script will create a new download list. The script can be set to run automatically as a cron job or be launched manually at any time. Currently, PlanetServer's download scripts are launched manually twice a year or after a major update of the PDS archive has been announced. The downloading scripts are available in our GitHub repository. The data are stored according to the volume they belong to (e.g `mrocr_2010`, `mrocr_2011`, etc). The data are then processed using CAT routines on ENVI. Several CAT IDL routines have been altered to automate the process and make them non-interactive, allowing us to run the process in the background. The result are atmospherically corrected and map projected CRISM images. The output IMG files are transformed into GeoTIFF using GDAL in order to be ingested into `rasdaman`. In the transformation process the metadata is kept in its original format in order to be used later by the ingestion script. Ingesting data into `rasdaman` can be easily performed by creating a so called ingredient (a json structured file descriptor) (Listing 2) and using the built-in routine `wcst_import`. In the ingredient, information related to the CRS, WMS capabilities, band nomenclature and null values are included. The `wcst_import` routine will read the ingredient parameters and depending on those ingest the data in one of the several possible ways. In this case a map mosaic mode ingredient with WMS enabled has been chosen. We also renamed the bands by a more convenient nomenclature as the name will be used when building the WCPS queries. Once the ingredients are created, the data are ingested into `petascope`. This data can be easily queried using either WMS, WCS or WCPS OGC standards.

M3. M3 data are also downloaded directly from PDS using a set of scripts. In this case we downloaded L1B and L2 data. L2 data contains thermally corrected reflectance data which is the data we are interested in. The reason of downloading both data levels is that the L2 data needs to be re-projected using Integrated Software for Imagers and Spectrometers (ISIS) (Gaddis et al. (1997) and Torson and Becker (1997)) routines and they are currently only available for L1B data. It appears that the reflectance file has the same characteristics (lines, samples, bands, bit type) as the M3 L1B data. A method has been found to change the L1B data label file to point into the L2 reflectance data (Hare, T., personal communication (2016)). This allows us to run the ISIS routine "cam2map" to reproject L2 data by using the L1B data label file. The pipeline

script containing all the necessary ISIS routines is launched in order to obtain the L2 map projected data. The data is transformed to GeoTIFF using GDAL for the same reason as in section 2.3.1. The only differences in the M3 ingestion ingredients are the CRS URL (pointing to Moon based CRSs) and the number of bands. As soon as higher level and/or re-calibrated data are available, they will be added or substitute the current data products.

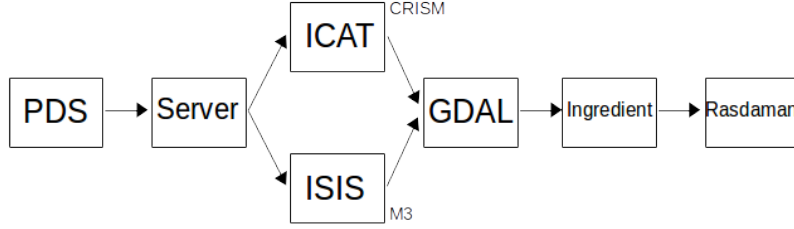


Figure 5: Pipeline for processing CRISM and M3 data. Both pipelines share some steps such as the GeoTIFF transformation while some parts of the pipeline are dataset tied.

Planetary CRS. Allowing full support of non-terrestrial CRS in web-based GIS is an ongoing effort among planetary scientists. Some proposals have been carried out (Rossi et al. (2016)) although no CRS have been yet included. Currently, the official CRS is defined by the International Astronomical Union (IAU) in 2000, named MARS2000. The MARS2000 definition consists of an ellipsoid with a 3396190 meter semi-major axis and a 3376200 meter semi-minor axis. As this definition is planetocentric, different from the terrestrial CRS which are planetographic, MARS2000 is not to be supported by many GIS clients (Oosthoek et al. (2014)). In order to solve this issue we defined the Martian CRS as a 3396190 meters ellipsoid with no flattening.

SECORE is the CRS resolver used by rasdaman. The CRS is developed in GML 3.2.1, validated and included into SECORE using its front-end web version, which will create a unique URL pointing to the CRS. The URL is included in the ingredients in order to define the CRS of the images while ingesting into rasdaman. For earth-based data, most of the CRS used are stored in opengis.net with their own unique URL. We created the CRS needed in PlanetServer and included them in SECORE. We defined ten CRS: 4 for Mars and 6 for the Moon. The list of CRSs and their unique URL can be found in Table 3 in the Appendix.

2.4. Examples

Mineral characterization in Mars is an ongoing research. Several studies of deposition and alteration phases have been carried out in different locations of the planet (Mustard et al. (2008), Carter et al. (2013a), Spectrometer (2005)). We carried out a study of the characterization of chlorite, prehnite and kaolinite in the Nili Fossae area, thus allowing us to compare the results obtained with PlanetServer to previous studies (Ehlmann et al. (2009) and Viviano-Beck et al. (2014)).

2.4.1. Chlorite and Prehnite

Chlorites are phyllosilicates formed by hydrothermal, metamorphic and diagenetic reactions (Ehlmann et al. (2009)). Prehnite, which usually appears in association with chlorite and pumpellyite, is a calcium aluminum silicate hydroxide material formed after hydrothermal or metamorphic activity. Chlorite shows a strong absorption band centered at 2.33 - 2.35 μm which combined with a shoulder at 2.26 μm distinguishes chlorites from serpentines. Prehnite shows also an absorption band centered at 2.35 - 2.36 μm coinciding with Fe-rich chlorites. An absorption band at 1.48 μm is uniquely related with the presence of prehnite.

Figure 6 shows a crater in the Nili Fossae area (17°N, 72°E) with a high chlorite content region. In Ehlmann et al. (2009) the combination used to characterize chlorite and prehnite (red: BD2350; green: D2300; blue: BD2200) have been derived from Pelkey et al. (2007) and show a distribution of chlorite/prehnite and K mica materials. In our study the images are obtained as a combination of three products (red: BD2355; green: D2300; blue: MIN2200) from Viviano-Beck et al. (2014) which are equivalent products. Chlorite and prehnite materials are shown in yellow in Figure 6 and are mainly located in the central part of the crater.

The spectral analysis, shown in Figure 6A, B and C, corroborates the presence of chlorites and prehnites. Figure 6A shows in blue the numerator (using a 3x3 kernel) where the absorption bands at 1.9 μm and 2.35 μm are already very prominent. The ratioed CRISM graph (Figure 6B) enhances the above mentioned absorption bands. Absorption bands at 1.48, 1.9 and 2.35 μm are associated with the presence of chlorite and prehnite, therefore we can say that the analyzed area contains chlorite, prehnite and pumpellyite. The graphs are compared against laboratory samples spectra included in the spectral library splib06a (Clark et al. (2007)) in order to validate the spectral analysis (Figure 6C).

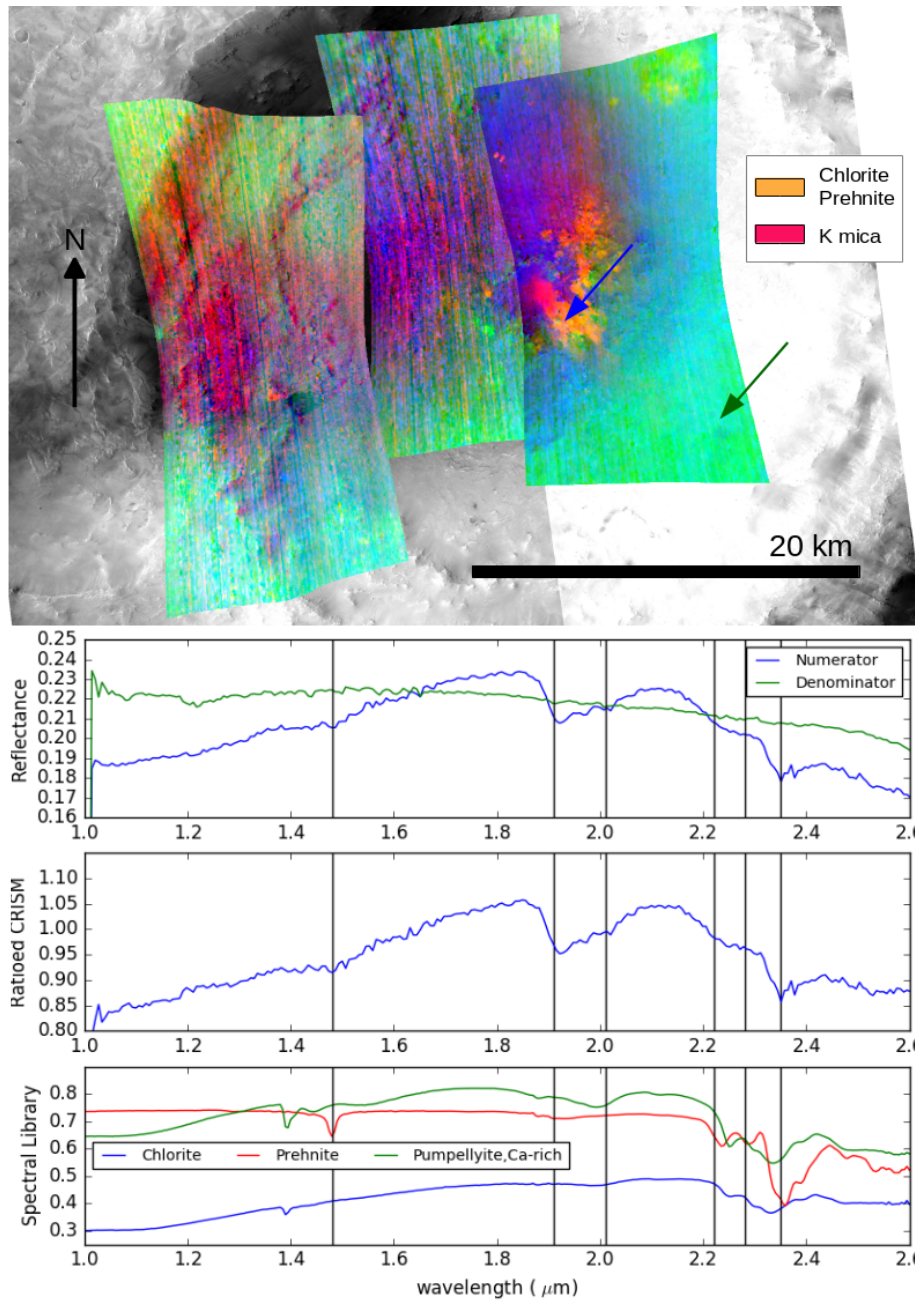


Figure 6: Chlorite in Toro crater within Nili Fossae. The RGB combination has been calculated using R: BD2355; G: D2300; B: MIN2200 which highlights the possible presence of chlorite in yellow. Raw spectra (Figure 6A) has been collected from the image FRT0000B1B5. The numerator (blue arrow) is located at 17.00813°N, 71.85837°E and the denominator (green arrow) at 16.91249°N, 71.99203°E. The ratioed spectra is shown in Figure 6B. Spectral analysis (Figure 6C) shows a mix of chlorite and prehnite with absorption bands at 1.48 μm , 2.22 μm , 2.28 μm and 2.35 μm . A clear mix of prehnite with hydrated minerals is present hence the absorption band at 1.9 μm . The shape of the continuum between 2.2 μm and 2.3 μm and after 2.5 μm suggests a putative mixture with either chlorite and/or pumpellyite.

2.4.2. Kaolinite

Kaolinites are a clay mineral including kaolinite, dickite, nacrite, montmorillonite and halloysite. Kaolinite is formed as a result of hydrothermal alteration and pedogenesis while halloysite is formed as a result of hydrothermal or weathering processes. Kaolinites show a strong absorption band at $1.4\text{ }\mu\text{m}$ and $2.2\text{ }\mu\text{m}$. An absorption band at $1.9\text{ }\mu\text{m}$ is also present but shows a variation in strength. Nacrite and Dickite show a distinct absorption band at $2.17\text{ }\mu\text{m}$. An absorption band at $1.92\text{ }\mu\text{m}$ is also visible which corresponds to halloysites.

Kaolinite is not as widely detected as chlorites but some traces of it can be found in Nili Fossae (Brown et al. (2010) and Ehlmann et al. (2009)) and other areas (? and Cuadros and Michalski (2013)). Figure 7 shows a small crater of around 5km diameter with a high content of Kaolinite (yellow) in its south-easternmost part of the rim (21°N , 73°E). The images are obtained after adapting the CRISM products from Pelkey et al. (2007) used in Ehlmann et al. (2009) (red: BD1900H; green: BD2200; blue: D2300) to the more actual developed by Viviano-beck (red: BD1900_2; green: MIN2200; blue:D2300). Such products are used to characterize kaolinite and smectite materials.

Smectite is shown in pink while kaolinites are shown in yellow and light-green. Note the high noise content present in Figure 7 which is also shown in a more dark green. It is mainly due to the fact that the absorption band corresponding to the green channel is near to the noise level in CRISM images. Applying image processing techniques such as calculating the median and dividing by it to reduce the noise will give us a less noise image but will also reduce the absorption band at $2.17\text{ }\mu\text{m}$. We decided to use the CRISM products without post-processing the image and further investigate the consequences of applying such filters in the results.

Figure 7A shows in blue the reflectance of the numerator where already absorption bands at 1.4 and $2.2\text{ }\mu\text{m}$ can be easily recognized. The ratioed CRISM (Figure 7B) increases its signal making it easier to recognize the absorption band at $1.92\text{ }\mu\text{m}$. The above mentioned absorption bands are tied to the presence of kaolinite, smectite, montmorillonite, nacrite, dickite and halloysite. As in the section 2.4.1, all the results are compared against laboratory samples included in the spectral library splib06a which can be seen in Figure 7C.

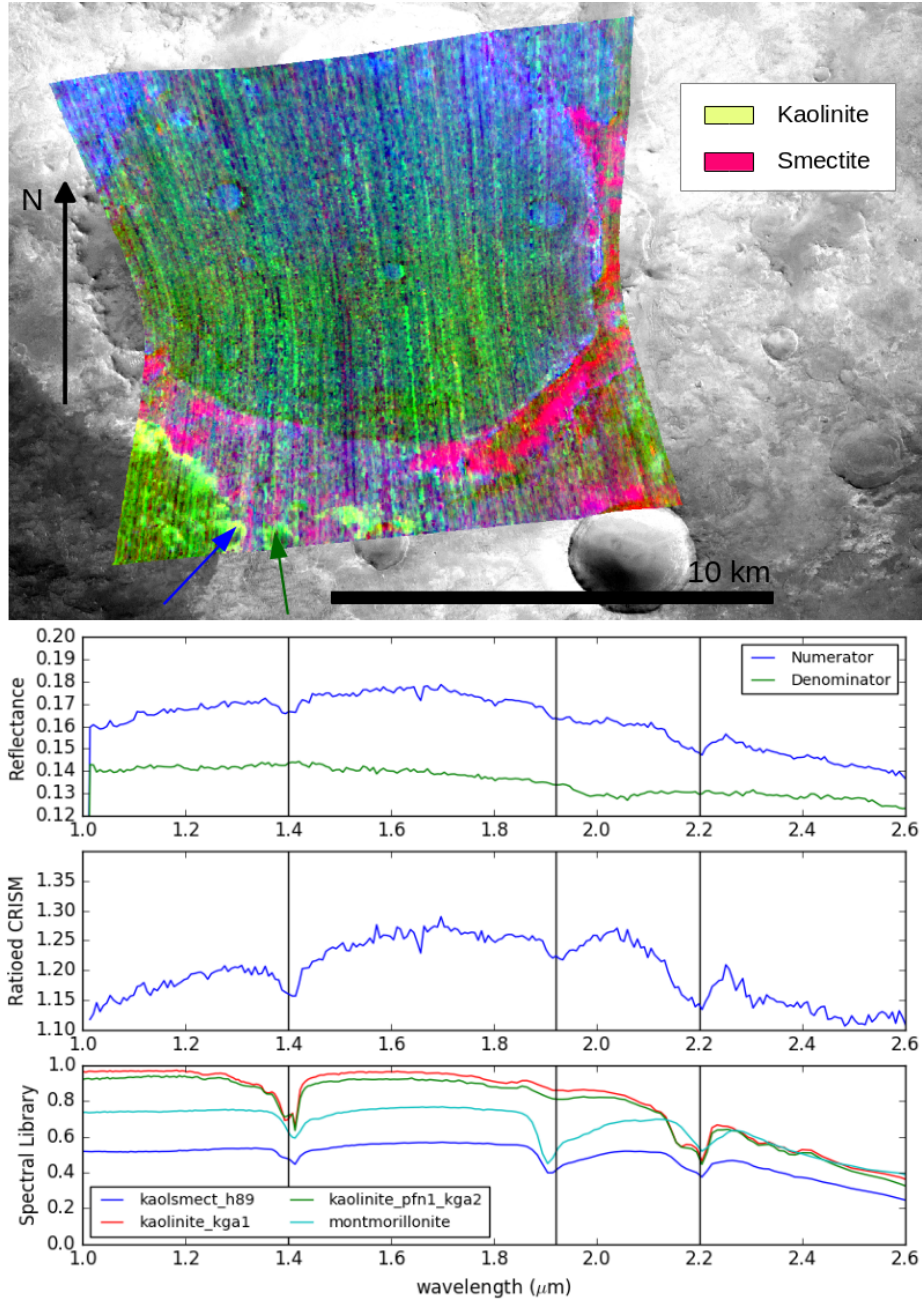


Figure 7: Kaolinite found in the image FRT0000C202 located in Nili Fossae. The RGB combination has been calculated using R: BD1900_2; G: MIN2200; B:D2300. A) Spectra collected at 21.17468°N, 73.31922°E (numerator, blue arrow) and 21.16931°N, 73.33749°E (denominator, green arrow) is shown. The ratioed (B) spectra of the numerator and denominator in A is presented. The vertical lines at 1.4, 1.92, and 2.2 mm correspond to absorption bands related with kaolinite, halloysite or kaolinite smectite clays. As seen in C the CRISM spectra has a better fit to kaolinite rather than montmorillonite as it coincides with the characteristic 2.16 μm absorption band found in kaolinites.

3. Discussion

PlanetServer is presented in this work as a work in process open-source and reproducible alternative to visualize and analyze hyperspectral images. The main use case is linked to Mars, but the applicability of code, tools and workflow is general purpose enough to be applied to other Solar System bodies and Earth Observation. The cross validation and the scientific results show the robustness of PlanetServer; further validation is planned. The scientific results are compared to previous studies (Ehlmann et al. (2009), Viviano-Beck et al. (2014)). Same minerals have been characterized with positive results. All the process is pursued in the same environment without having to know specifically any of the OGC standards, WCPS specially. As the client (Marco Figuera (2016)) is open-source and available in GitHub¹⁶, it is easy to modify and add more CRISM products and WCPS queries.

As all the products can be downloaded, the results obtained in PlanetServer (images and plots) can be easily included in scientific publications. Giving the fact that PlanetServer and rasdaman Community edition¹⁷ are open-source, both the client and the database manager can be deployed in another system in order to serve different datasets. PlanetServer contributes towards cost-effective workflows as it is not required to pay any licenses for a fully functional setup.

3.1. Ongoing work

Ongoing work includes the development of a Python API. The API will help in the creation of all the CRISM products mentioned in (Viviano-Beck et al., 2014). It will only need four input arguments: Coverage Identification and the name of 3 CRISM products to be stored in each channel. The output will be an image with the given parameters. The inclusion of spectral analysis in the API is being evaluated. Once the API is published we will provide a set of Jupyter Notebooks in order to give an overview of its capabilities. An early stage of PlanetServer working on a Jupyter notebook is already accessible¹⁸.

New datasets are being considered. The CRISM MRDR dataset (McGuire et al. (2013)) will be shortly included in PlanetServer and will allow the possibility to analyze bigger areas with one WCPS query. The CRISM MRDR dataset is composed by a set of mosaics served as tiles covering the whole Martian surface¹⁹.

New M3 data is being processed to be ingested in the Lunar client. The reason of using the pipeline described in section 2.3.1 is to apply the thermal correction of L2 data into L1B data and process the data using ISIS routines. We found out that, while some images are processed without any error, some images appear to be corrupted during the process. Further investigations are being taken in order to analyze and solve the issue. An hypothesis of the error

¹⁶<https://github.com/planetserver/ps2-www-client>

¹⁷<http://rasdaman.org/>

¹⁸https://github.com/earthserver-eu/INSPIRE-notebooks/blob/master/ps2_inspire_notebook.ipynb

¹⁹http://pds-geosciences.wustl.edu/missions/mro/090220.current_if_tru.png

source could be the hacking of the label files which corrupts the ISIS3 procedure. Once the M3 data is processed we will achieve a nearly global M3 coverage.

The inclusion of topographic datasets is also being evaluated and tested using High Resolution Stereo Camera (HRSC, Mars Express) data (Jaumann et al. (2015)). PlanetServer will include a set of DTMs for all the planetary bodies as well as a set of tools to pursue topographic analysis - traverse, roughness, slopes and aspects. A possible application of including topographic analysis to the current tools is landing site characterization (Golombek et al. (2007) and Golombek et al. (2003)). The Java Mission-planning and Analysis for Remote Sensing (JMARS) (Christensen et al. (2009)) is a software developed in Java allowing the user to plan and process landing site selection analysis. While JMARS is a very powerful tool it needs to be downloaded and run locally. Including the topographic tools, a set of illumination maps (Figuera et al. (2014) and Marco Figuera et al. (2016)) and the existing analytical tools will grant PlanetServer to be an online alternative for Landing site selection.

Discussions have started in order to evaluate the inclusion of OMEGA data for Mars and Messenger data for Mercury. Future plans for the inclusion of a hyperspectral clustering tool in PlanetServer using a server based python API is being evaluated. The inclusion of this feature needs to be further evaluated as it will increase the stress in the servers.

Efforts are being made in order to standardize the declaration of IAU CRSs and include them in opengis (Rossi et al. (2016)).

4. Conclusions

The results obtained in this research demonstrates PlanetServer as a reliable tool for the visualization and analysis of hyperspectral data. Several investigations have been pursued in order to validate our products giving a positive result in all the tests. It has been proved the reliability of PlanetServer in the analysis of spectra and the visualization of images and band math combinations. The fact of having an all-in-one platform provides us the possibility of running quick tests in a very short time. As an example, the cross validation of the chlorites and prehnites products was completed in just one hour based on the investigation pursued by Ehlmann et al. (2009). Once the cross validation of the chlorites was finished, finding new areas with chlorite and prehnite was a routine process comparable to those done by using other software such as ENVI.

PlanetServer can be easily integrated in Python providing us the possibility to make use of all the libraries present in Python. This extends the power of PlanetServer for the analysis of CRISM images. The python API can be easily integrated and combined with existing geo-libraries such as gdal, providing the possibility of map mosaic the results.

The combination of OGC standards, open-source server and client tools as well as openly available algorithms together with WCPS versions of hyperspectral formulas allows reproducibility of scientific observations and surface mapping. We need a joint effort including universities, companies and space

agencies in order to lead the development of new tools into a more openly and easily accessible philosophy. It is proved that by making accessible tools to analyze planetary data we can reduce time and budget spent in developing custom tools and focus on the analysis and the scientific output.

Acknowledgments

The EarthServer-2 project receives funding from the European Unions Horizon 2020 research and innovation program under the grant agreement No 654367 (e-Infrastructures). The authors wish to thank the CLAMV team (Achim Gellusus, Florian Neu) to let us and help us into using the cluster, the L-sis group (Vlad Merticariu, Alex Dumitru and Dimitar Misev) for all their help in rasdaman related issues. We thank Melissa Martinot for helping finding laboratory spectra samples. We would like to thank Trent Hare for its help creating the M3 pipeline and for a all the information regarding CRSs. Also, we would like to thank the EarhtServer-2 Consortium as a whole and particularly its Service Partners for the valuable discussions and for their help.

5. Appendix

Table 3 shows a list of all the available CRS created in PlanetServer and stored in SECORE. The CRS are created in XML format and added to SECORE using its web interface. The CRS's correctness is checked by SECORE prior ingestion.

Table 4 shows the location in degrees of all the locations used in section 2.4. Images below 65 use equirectangular projection and above 65 polar stereographic projection.

Table 4: Location of Numerators and Denominators used in Figures 7 and 8

Label	Location		Image ID in PlanetServer
	Latitude	Longitude	
Figure 6			
Numerator	17.00813	71.85837	frt0000b1b5_07_if165l_trr3
Denominator	16.91249	71.99203	hrl000086ca_07_if182l_trr3
Figure 7			
Numerator	21.17468	73.31922	frt0000c202_07_if165l_trr3
Denominator	21.16931	73.33749	frt0000c202_07_if165l_trr3

Table 5 shows a detailed list of the laboratory spectra used to analyze the CRISM spectra in section 2.4.

Table 3: List of URLs of available CRSs in PlanetServer

Body	CRS	URL
Mars		
	Mars Equirectangular	http://access.planetserver.eu:8081/def/crs/PS/0/Mars-equirectangular
	Mars Geographic	http://access.planetserver.eu:8081/def/crs/PS/0/Mars-geographic
	Mars North polar stereographic	http://access.planetserver.eu:8081/def/crs/PS/0/Mars-stereographic-north
	Mars South polar stereographic	http://access.planetserver.eu:8081/def/crs/PS/0/Mars-stereographic-south
Moon		
	Moon Equirectangular	http://access.planetserver.eu:8081/def/crs/PS/0/Moon-equirectangular
	Moon Geographic	http://access.planetserver.eu:8081/def/crs/PS/0/Moon-geographic
	Moon North polar stereographic	http://access.planetserver.eu:8081/def/crs/PS/0/Moon-gnomonic-north
	Moon South polar stereographic	http://access.planetserver.eu:8081/def/crs/PS/0/Moon-gnomonic-south
	Moon North polar gnomonic	http://access.planetserver.eu:8081/def/crs/PS/0/Moon-stereographic-north
	Moon South polar gnomonic	http://access.planetserver.eu:8081/def/crs/PS/0/Moon-stereographic-south

Table 5: List of sample names and sources used in Figures 4-7.

Label	Sample ID	Source
Figure 7		
Chlorite	c2cl14_bdvnr	PDS Geoscience Spectral Library
Prehnite	c1ze03_bdvnr	PDS Geoscience Spectral Library
Pumpellyite,Ca-rich	c1ze01_bdvnr	PDS Geoscience Spectral Library
Figure 8		
kaolsmect_h89	kaolsmect_h89fr2.25636	splib06a
kaolinite_kga1	kaolinite_kga1.12117	splib06a
kaolinite_pfn1_kga2	kaolinite_pfn1_kga2.12176	splib06a
montmorillonite	montmorillonite.swy1.14688	splib06a

Example of ingredient used for the ingestion of a CRISM image:

Listing 2: Ingredient used in PlanetServer to ingest a CRISM image in the Rasdaman database.

```

1  {
2    "config": {
3      "service_url": "http://localhost:8080/rasdaman/ows",
4      "tmp_directory": "/tmp",
5      "crs_resolver": "http://localhost:8080/def",
6      "default_crs": "http://localhost:8080/def/crs/PS/0/Mars-
7        equirectangular",
8      "subset_correction": false,
9      "mock": false,
10     "automated": true
11   },
12   "input": {
13     "coverage_id": "frt00005f1f_07_if163l_trr3",
14     "paths": [
15       "../frt00005f1f_07_if163l_trr3-CAT_scale_trial-p.img.tif"
16     ]
17   },
18   "recipe": {
19     "name": "map_mosaic",
20     "options": {
21       "tiling": "ALIGNED_[0:1023,0:1023]_TILE_SIZE_4194304",
22       "wms_import": true,
23       "band_names": [
24         "band_1",
25         "band_2",
26         "band_3",
27         "band_4",

```

```

38 "band_5",
39 .
40 .
41 .
42 "band_438"
43     ]
44     }
45 }
46 }

```

A list of different WCPS queries is provided. The following query is used to retrieve spectra profiles from CRISM images:

Listing 3: Single pixel spectra query

```

for c in (frt0000a0ac_07_if165l_trr3) return encode( c[ N
(1277.941354035707:1277.941354035707), E
(1022.353146921535:1022.353146921535) ], "csv")

```

The following WCPS query is used to create a false color RGB combination. This query is used as the default RGB combination when an image is selected.

Listing 4: RGB false color WCPS query

```

for data in (frt0000a0ac_07_if165l_trr3) return encode( {
red: (float)((int)(255 / (max( data.band_233) - min(data.band_233))
) * (data.band_233 - min(data.band_233)));
green: (float)((int)(255 / (max( data.band_13) - min(data.band_13))
) * (data.band_13 - min(data.band_13)));
blue: (float)((int)(255 / (max( data.band_78) - min(data.band_78))
) * (data.band_78 - min(data.band_78))) ;
alpha: (float)((data.band_100 > 0) * 255)}, "png", "nodata=65535")

```

The following query creates the HYD browse product from Viviano-Beck et al. (2014). The first stretching to translate the indexes to the PNG range is added in the query.

Listing 5: Viviano-beck HYD CRISM product WCPS query

```

for data in ( frt0000a0ac_07_if165l_trr3 ) return encode( {
Red:(float)((int)( 255 / ( max((1 - ((1 - (0.607142857))*data.
band_171 + (0.607142857)*data.band_213)/(data.band_197))) - min
((1 - ((1 - (0.607142857))*data.band_171 + (0.607142857)*data.
band_213)/(data.band_197))) ) ) * ( ((1 - ((1 - (0.607142857))*
data.band_171 + (0.607142857)*data.band_213)/(data.band_197)))
- min((1 - ((1 - (0.607142857))*data.band_171 + (0.607142857)*
data.band_213)/(data.band_197))) ) ));
Green:(float)((int)( 255 / ( max((1 - ((data.band_173) / ((1 -
(0.63125)) * data.band_142 + (0.63125) * data.band_191)))) -
min((1 - ((data.band_173) / ((1 - (0.63125)) * data.band_142 +
(0.63125) * data.band_191)))) ) ) * ( ((1 - ((data.band_173) /
((1 - (0.63125)) * data.band_142 + (0.63125) * data.band_191)))
- min((1 - ((data.band_173) / ((1 - (0.63125)) * data.
band_142 + (0.63125) * data.band_191)))) ) ));
Blue:(float)((int)( 255 / ( max((0.5 * (1 - ((data.band_142) / ((1
- (0.36346516)) * data.band_130 + (0.36346516) * data.band_163)
)) * 0.5 * (1 - ((data.band_151) / ((1 - (0.636167379)) * data.
band_130 + (0.636167379) * data.band_163)))))) - min((0.5 * (1 -
((data.band_142) / ((1 - (0.36346516)) * data.band_130 +

```

```

(0.36346516) * data.band_163))) * 0.5 * (1 - ((data.band_151) /
((1 - (0.636167379)) * data.band_130 + (0.636167379) * data.
band_163)))))) * ( ((0.5 * (1 - ((data.band_142) / ((1 -
(0.36346516)) * data.band_130 + (0.36346516) * data.band_163)))
* 0.5 * (1 - ((data.band_151) / ((1 - (0.636167379)) * data.
band_130 + (0.636167379) * data.band_163)))))) - min((0.5 * (1 -
((data.band_142) / ((1 - (0.36346516)) * data.band_130 +
(0.36346516) * data.band_163))) * 0.5 * (1 - ((data.band_151) /
((1 - (0.636167379)) * data.band_130 + (0.636167379) * data.
band_163)))))) ));
alpha: (data.band_100 > 0) * 255 }, "tiff", "nodata=65535")

```

References

- Aiordchioaie, A., Baumann, P., 2010. PetaScope: An open-source implementation of the OGC WCS Geo service standards suite. Lecture Notes in Computer Science (including subseries Lecture Notes in Artificial Intelligence and Lecture Notes in Bioinformatics) 6187 LNCS, 160–168. URL: <http://dl.acm.org/citation.cfm?id=1876037.1876053>, doi:10.1007/978-3-642-13818-8{_}13.
- Baumann, P., 2010. The OGC web coverage processing service (WCPS) standard. *GeoInformatica* 14, 447–479. URL: <http://dl.acm.org/citation.cfm?id=1831146.1831160>, doi:10.1007/s10707-009-0087-2.
- Baumann, P., Dehmel, A., Furtado, P., Ritsch, R., Widmann, N., 1998. The multidimensional database system RasDaMan. *ACM SIGMOD Record* 27, 575–577. URL: <http://dl.acm.org/citation.cfm?id=276305.276386>, doi:10.1145/276305.276386.
- Baumann, P., Mazzetti, P., Ungar, J., Barbera, R., Barboni, D., Beccati, A., Bigagli, L., Boldrini, E., Bruno, R., Calanducci, A., Campalani, P., Clements, O., Dumitru, A., Grant, M., Herzig, P., Kakaletis, G., Laxton, J., Koltsida, P., Lipskoch, K., Mahdiraji, A.R., Mantovani, S., Merticariu, V., Messina, A., Misev, D., Natali, S., Nativi, S., Oosthoek, J., Pappalardo, M., Passmore, J., Rossi, A.P., Rundo, F., Sen, M., Sorbera, V., Sullivan, D., Torrisi, M., Trovato, L., Veratelli, M.G., Wagner, S., 2015. Big Data Analytics for Earth Sciences: the EarthServer approach. *International Journal of Digital Earth* 8947, 1–27. URL: <http://www.tandfonline.com/doi/abs/10.1080/17538947.2014.1003106>, doi:10.1080/17538947.2014.1003106.
- Bibring, J.P., Langevin, Y., Mustard, J.F., Poulet, F., Arvidson, R., Gendrin, A., Gondet, B., Mangold, N., Pinet, P., Forget, F., Berthé, M., Bibring, J.P., Gendrin, A., Gomez, C., Gondet, B., Jouglet, D., Poulet, F., Soufflot, A., Vincendon, M., Combes, M., Drossart, P., Encrenaz, T., Fouchet, T., Mercurio, R., Belluci, G., Altieri, F., Formisano, V., Capaccioni, F., Ceroni, P., Coradini, A., Fonti, S., Korabely, O., Kottsov, V., Ignatiev, N., Moroz, V., Titov, D., Zasova, L., Loiseau, D., Mangold, N., Pinet, P., Douté, S., Schmitt, B., Sotin, C., Hauber, E., Hoffmann, H., Jaumann, R., Keller, U.,

- Arvidson, R., Mustard, J.F., Duxbury, T., Forget, F., Neukum, G., 2006. Global Mineralogical and Aqueous Mars History Derived from OMEGA/Mars Express Data. *Science* 312, 400–404. URL: <http://science.sciencemag.org/content/312/5772/400.abstract>, doi:10.1126/science.1122659.
- Bibring, J.P., Soufflot, A., Berthé, M., Langevin, Y., Gondet, B., Drossart, P., Bouy, M., Combes, M., Puget, P., Semery, A., Bellucci, G., Formisano, V., Moroz, V., Kottsov, V., Bonello, G., Erard, S., Forni, O., Gendrin, A., Manaud, N., Poulet, F., Poulleau, G., Encrenaz, T., Fouchet, T., Melchiori, R., Altieri, F., Ignatiev, N., Titov, D., Zasova, L., Coradini, A., Capacionni, F., Cerroni, P., Fonti, S., Mangold, N., Pinet, P., Schmitt, B., Sotin, C., Hauber, E., Hoffmann, H., Jaumann, R., Keller, U., Arvidson, R., Mustard, J., Forget, F., 2004. OMEGA: Observatoire pour la minéralogie, l’eau, les glaces et l’activité. European Space Agency, (Special Publication) ESA SP 1240, 37—49.
- Brown, A.J., Hook, S.J., Baldridge, A.M., Crowley, J.K., Bridges, N.T., Thomson, B.J., Marion, G.M., de Souza Filho, C.R., Bishop, J.L., 2010. Hydrothermal formation of Clay-Carbonate alteration assemblages in the Nili Fossae region of Mars. doi:10.1016/j.jeps.2010.06.018, arXiv:1402.1150.
- Carter, J., Poulet, F., Bibring, J.P., Mangold, N., Murchie, S., 2013a. Hydrous minerals on Mars as seen by the CRISM and OMEGA imaging spectrometers: Updated global view. *Journal of Geophysical Research E: Planets* 118, 831–858. URL: <http://doi.wiley.com/10.1029/2012JE004145>, doi:10.1029/2012JE004145.
- Carter, J., Poulet, F., Murchie, S., Bibring, J., 2013b. Automated processing of planetary hyperspectral datasets for the extraction of weak mineral signatures and applications to CRISM observations of hydrated silicates on Mars. *Planetary and Space Science* 76, 53–67. URL: <http://www.sciencedirect.com/science/article/pii/S0032063312003625>, doi:10.1016/j.pss.2012.11.007.
- Chiwome, V., 2014. Webclient-neo: Planetserver/Earthserver project end. Zenodo doi:10.5281/zenodo.11698.
- Christensen, P.R., Engle, E., Anwar, S., Dickenshied, S., Noss, D., Gorelick, N., Weiss-Malik, M., 2009. JMARS - A Planetary GIS. American Geophysical Union, Fall Meeting 2009, abstract #IN22A-06 URL: <http://adsabs.harvard.edu/abs/2009AGUFMIN22A..06C>.
- Clark, R.N., Swayze, G.A., Wise, R., Livo, E., Hoefen, T., Kokaly, R., Sutley, S.J., 2007. USGS digital spectral library splib06a: U.S. Geological Survey, Digital Data Series 231. URL: <http://speclab.cr.usgs.gov/spectral.lib06>.
- Cuadros, J., Michalski, J.R., 2013. Investigation of Al-rich clays on Mars: Evidence for kaolinite-smectite mixed-layer versus mixture of end-member phases. *Icarus* 222, 296–306. doi:10.1016/j.icarus.2012.11.006.

- Day, B.H., Law, E.S., 2016. Moon Trek: NASA's new online portal for lunar mapping and modeling, in: Annual Meeting of the Lunar Exploration Analysis Group. URL: <http://www.hou.usra.edu/meetings/leag2016/pdf/5015.pdf>.
- Ehlmann, B.L., Mustard, J.F., Swayze, G.A., Clark, R.N., Bishop, J.L., Poulet, F., Des Marais, D.J., Roach, L.H., Milliken, R.E., Wray, J.J., Barnouin-Jha, O., Murchie, S.L., 2009. Identification of hydrated silicate minerals on Mars using MRO-CRISM: Geologic context near Nili Fossae and implications for aqueous alteration. *Journal of Geophysical Research E: Planets* 114, E00D08. URL: <http://doi.wiley.com/10.1029/2009JE003339>, doi:10.1029/2009JE003339.
- Erkeling, G., Luesebrink, D., Hiesinger, H., Reiss, D., Heyer, T., Jaumann, R., 2016. The Multi-Temporal Database of Planetary Image Data (MUTED): A database to support the identification of surface changes and short-lived surface processes, in: *Planetary and Space Science*, pp. 43–61. URL: <http://www.hou.usra.edu/meetings/lpsc2016/pdf/1852.pdf>, doi:10.1016/j.pss.2016.03.002.
- Figuera, R.M., Gläser, P., Oberst, J., De Rosa, D., 2014. Calculation of illumination conditions at the lunar south pole - parallel programming approach, in: *European Planetary Science Congress 2014, EPSC Abstracts*, Vol. 9, id. EPSC2014-476, pp. EPSC2014-476. URL: <http://adsabs.harvard.edu/abs/2014EPSC...9..476F>.
- Gaddis, L., Anderson, J., Becker, K., Cook, D., Edwards, K., Eliason, E., Hare, T., Kieffer, H., Lee, E.M., Matthews, J., 1997. An overview of the Integrated Software for Imaging Spectrometers (ISIS). *Lunar and planetary science XXVIII* 28, 1997.
- Gaskins, T.O.M., 2009. Spatial Information Processing : Standards-Based Open Source Visualization Technology, in: *Data Processing*, pp. 1–3. URL: http://www.isprs.org/proceedings/xxxviii/4-w10/papers/vcgva2009_{_}03307{_{_}hogan.pdf.
- van Gasselt, S., Morley, J.G., Houghton, R., Bamford, S., Ivanov, A., Muller, J.P., Yershov, V., Sidiropoulos, P., Gwinner, K., Wählisch, M., Kim, J.R., 2014. The iMars WebGIS A Central Hub for Displaying and Distributing Co-Registered Data of Mars, in: *European Planetary Science Congress 2014*. doi:EPSC2014-693.
- Golombek, M., Grant, J., Vasavada, A.R., Watkins, M., 2007. Landing Sites Proposed for the Mars Science Laboratory Mission. 38th Lunar and Planetary Science Conference, (Lunar and Planetary Science XXXVIII), held March 12–16, 2007 in League City, Texas. LPI Contribution No. 1338, p.1392 38, 1392. URL: <http://adsabs.harvard.edu/abs/2007LPI....38.1392G>.

- Golombek, M.P., Grant, J.A., Parker, T.J., Kass, D.M., Crisp, J.A., Squyres, S.W., Haldemann, A.F.C., Adler, M., Lee, W.J., Bridges, N.T., Arvidson, R.E., Carr, M.H., Kirk, R.L., Knocke, P.C., Roncoli, R.B., Weitz, C.M., Schofield, J.T., Zurek, R.W., Christensen, P.R., Fergason, R.L., Anderson, F.S., Rice, J.W., 2003. Selection of the Mars Exploration Rover landing sites. *Journal of Geophysical Research: Planets* 108. URL: <http://doi.wiley.com/10.1029/2003JE002074>, doi:10.1029/2003JE002074.
- Green, R.O., Pieters, C., Mouroulis, P., Eastwood, M., Boardman, J., Glavich, T., Isaacson, P., Annadurai, M., Besse, S., Barr, D., Buratti, B., Cate, D., Chatterjee, A., Clark, R., Cheek, L., Combe, J., Dhingra, D., Essandoh, V., Geier, S., Goswami, J.N., Green, R., Haemmerle, V., Head, J., Hovland, L., Hyman, S., Klima, R., Koch, T., Kramer, G., Kumar, A.S.K., Lee, K., Lundeen, S., Malaret, E., McCord, T., McLaughlin, S., Mustard, J., Nettles, J., Petro, N., Plourde, K., Racho, C., Rodriguez, J., Runyon, C., Sellar, G., Smith, C., Sobel, H., Staid, M., Sunshine, J., Taylor, L., Thaisen, K., Tompkins, S., Tseng, H., Vane, G., Varanasi, P., White, M., Wilson, D., 2011. The Moon Mineralogy Mapper (M3) imaging spectrometer for lunar science: Instrument description, calibration, on-orbit measurements, science data calibration and on-orbit validation. *Journal of Geophysical Research E: Planets* 116, E00G19. URL: <http://doi.wiley.com/10.1029/2011JE003797>, doi:10.1029/2011JE003797.
- Hare, T.M., Keszthelyi, L., Gaddis, L., Kirk, R.L., 2014. Online Planetary Data and Services at USGS Astrogeology, in: *Lunar and Planetary Science Conference*, Vol. 45, p. 2487. URL: http://www.dlr.de/pf/Portaldata/6/Resources/dokumente/isprs_{_}2014/Hare_{_}MTSTC4-2014-135.pdf.
- Jaumann, R., Tirsch, D., Hauber, E., Ansan, V., Di Achille, G., Erkeling, G., Fueten, F., Head, J., Kleinhans, M., Mangold, N., Michael, G., Neukum, G., Pacifici, A., Platz, T., Pondrelli, M., Raack, J., Reiss, D., Williams, D., Adeli, S., Baratoux, D., de Villiers, G., Foing, B., Gupta, S., Gwinner, K., Hiesinger, H., Hoffmann, H., Deit, L.L., Marinangeli, L., Matz, K.D., Mertens, V., Muller, J., Pasckert, J., Roatsch, T., Rossi, A., Scholten, F., Sowe, M., Voigt, J., Warner, N., 2015. Quantifying geological processes on Mars Results of the high resolution stereo camera (HRSC) on Mars express. *Planetary and Space Science* 112, 53–97. URL: <http://linkinghub.elsevier.com/retrieve/pii/S0032063315000392>, doi:10.1016/j.pss.2014.11.029.
- Liu, Y., Glotch, T.D., Scudder, N.A., Kraner, M.L., Condus, T., Arvidson, R.E., Guinness, E.A., Wolff, M.J., Smith, M.D., 2016. End-member Identification and Spectral Mixture Analysis of CRISM Hyperspectral Data: A Case Study on Southwest Melas Chasma, Mars. *Journal of Geophysical Research: Planets*, 1–33 URL: <http://doi.wiley.com/10.1002/2016JE005028>, doi:10.1002/2016JE005028.
- Lozac'h, L., Quantin-Nataf, C., Allemand, P., Bultel, B., Clenet, H., Harrisson, S., Loizeau, D., Ody, A., Thollot, P., 2015. MARSSI: a distributed

- information system for managing data of the surface of mars, in: Second Planetary Data Workshop. URL: <http://www.hou.usra.edu/meetings/planetdata2015/pdf/7006.pdf>.
- Marco Figuera, R., 2016. PlanetServer web client doi:10.5281/zenodo.200371.
- Marco Figuera, R., Flahaut, J., Gläser, P., Williams, P., Rossi, A.P., 2016. Water ice characterization near candidate landing sites at the lunar south pole, in: European Lunar Symposium. URL: http://els2016.arc.nasa.gov/downloads/ELS{}_2016{}_Abstract{}_Booklet{}_v2.pdf.
- McGuire, P., Arvidson, R., Bishop, J., Brown, A., Cull, S., Green, R., Gross, C., Hash, C., Hauber, E., Humm, D., Jaumann, R., Le Deit, L., Malaret, E., Martin, T., Marzo, G., Morgan, M., Murchie, S., Mustard, J., Neukum, G., Parente, M., Platz, T., Roush, T., Seelos, F., Smith, M., Sowe, M., Tirsch, D., Walter, S., Wendt, L., Wiseman, S., Wolff, M., 2013. Mapping Minerals on Mars with CRISM: Atmospheric and Photometric Correction for MRDR Map Tiles, Version 2, and Comparison to OMEGA, in: 44th Lunar and Planetary Science Conference.
- McMahon, S.K., 1996. Overview of the Planetary Data System. *Planetary and Space Science* 44, 3–12. URL: <http://www.sciencedirect.com/science/article/pii/0032063395001018>, doi:10.1016/0032-0633(95)00101-8.
- Misev, D., Rusu, M., Baumann, P., 2012. A semantic resolver for coordinate reference systems. *Lecture Notes in Computer Science (including subseries Lecture Notes in Artificial Intelligence and Lecture Notes in Bioinformatics)* 7236 LNCS, 47–56. doi:10.1007/978-3-642-29247-7{}_5.
- Murchie, S., Arvidson, R., Bedini, P., Beisser, K., Bibring, J.P., Bishop, J., Boldt, J., Cavender, P., Choo, T., Clancy, R.T., Darlington, E.H., Des Marais, D., Espiritu, R., Fort, D., Green, R., Guinness, E., Hayes, J., Hash, C., Heffernan, K., Hemmler, J., Heyler, G., Humm, D., Hutcheson, J., Izenberg, N., Lee, R., Lees, J., Lohr, D., Malaret, E., Martin, T., McGovern, J.A., McGuire, P., Morris, R., Mustard, J., Pelkey, S., Rhodes, E., Robinson, M., Roush, T., Schaefer, E., Seagrave, G., Seelos, F., Silverglate, P., Slavney, S., Smith, M., Shyong, W.J., Strohbehn, K., Taylor, H., Thompson, P., Tossman, B., Wirzbürger, M., Wolff, M., 2007. Compact Connaissance Imaging Spectrometer for Mars (CRISM) on Mars Reconnaissance Orbiter (MRO). *Journal of Geophysical Research E: Planets* 112, E05S03. URL: <http://doi.wiley.com/10.1029/2006JE002682>, doi:10.1029/2006JE002682.
- Murchie, S.L., Mustard, J.F., Ehlmann, B.L., Milliken, R.E., Bishop, J.L., Mckewen, N.K., Dobrea, E.Z.N., Seelos, F.P., Buczkowski, D.L., Wiseman, S.M., Arvidson, R.E., Wray, J.J., Swayze, G., Clark, R.N., Marais, D.J.D., McEwen, A.S., Bibring, J.P., 2009. A synthesis of Martian aqueous mineralogy after 1 Mars year of observations from the Mars Reconnaissance Orbiter. *J. Geophys. Res* 114, 0–6. doi:10.1029/2009JE003342.

- Mustard, J.F., Murchie, S.L., Pelkey, S.M., Ehlmann, B.L., Milliken, R.E., Grant, J.a., Bibring, J.P., Poulet, F., Bishop, J., Dobrea, E.N., Roach, L., Seelos, F., Arvidson, R.E., Wiseman, S., Green, R., Hash, C., Humm, D., Malaret, E., McGovern, J.a., Seelos, K., Clancy, T., Clark, R., Marais, D.D., Izenberg, N., Knudson, a., Langevin, Y., Martin, T., McGuire, P., Morris, R., Robinson, M., Roush, T., Smith, M., Swayze, G., Taylor, H., Titus, T., Wolff, M., 2008. Hydrated silicate minerals on Mars observed by the Mars Reconnaissance Orbiter CRISM instrument. *Nature* 454, 305–309. URL: <http://www.nature.com/nature/journal/v454/n7202/pdf/nature07097.pdf>, doi:10.1038/nature07097.
- Oosthoek, J., Arriazu, P., Marco Figuera, R., 2015. Shall We Send Humans to Holden Crater? How a Geodesic GIS Approach Can Aid the Landing Site Selection for Future Missions to Mars. First Landing Site/Exploration Zone Workshop for Human Missions to the Surface of Mars 1879, 1049. URL: <http://adsabs.harvard.edu/abs/2015LPICo1879.10490>.
- Oosthoek, J., Flahaut, J., Rossi, A., Baumann, P., Misev, D., Campalani, P., Unnithan, V., 2014. PlanetServer: Innovative approaches for the online analysis of hyperspectral satellite data from Mars. *Advances in Space Research* 53, 1858–1871. URL: <http://www.sciencedirect.com/science/article/pii/S0273117713004134>, doi:10.1016/j.asr.2013.07.002.
- Pelkey, S.M., Mustard, J.F., Murchie, S., Clancy, R.T., Wolff, M., Smith, M., Milliken, R.E., Bibring, J.P., Gendrin, A., Poulet, F., Langevin, Y., Gondet, B., 2007. CRISM multispectral summary products: Parameterizing mineral diversity on Mars from reflectance. *Journal of Geophysical Research E: Planets* 112, E08S14. URL: <http://doi.wiley.com/10.1029/2006JE002831>, doi:10.1029/2006JE002831.
- Pieters, C.M., Boardman, J., Buratti, B., Chatterjee, A., Clark, R., Glavich, T., Green, R., Head III, J., Isaacson, P., Malaret, E., Mccord, T., Mustard, J., Petro, N., Runyon, C., Staid, M., Sunshine, J., Taylor, L., Tompkins, S., Varanasi, P., White, M., 2009. The Moon Mineralogy Mapper (M₃) on Chandrayaan-1. *CURRENT SCIENCE* 96.
- Poulet, F., Bibring, J.P., Mustard, J.F., Gendrin, A., Mangold, N., Langevin, Y., Arvidson, R.E., Gondet, B., Gomez, C., Berthé, M., Bibring, J.P., Langevin, Y., Erard, S., Forni, O., Gendrin, A., Gondet, B., Manaud, N., Poulet, F., Poulleau, G., Soufflot, A., Combes, M., Drossart, P., Encrenaz, T., Fouchet, T., Melchiorri, R., Bellucci, G., Altieri, F., Formisano, V., Fonti, S., Capaccioni, F., Cerroni, P., Coradini, A., Korablev, O., Kottsov, V., Ignatiev, N., Titov, D., Zasova, L., Mangold, N., Pinet, P., Schmitt, B., Sotin, C., Hauber, E., Hoffmann, H., Jaumann, R., Keller, U., Arvidson, R., Mustard, J., Forget, F., 2005. Phyllosilicates on Mars and implications for early martian climate. *Nature* 438, 623–627. URL: <http://www.nature.com/doifinder/10.1038/nature04274>, doi:10.1038/nature04274.

- Rossi, P., Hare, T., Baumann, P., Misev, D., Marmo, C., Erard, S., Cecconi, B., Marco Figuera, R., 2016. Planetary Coordinate Reference Systems for Ogc Web Services. a, in: 47th Lunar and Planetary Science Conference.
- Spectrometer, R., 2005. Mars Surface Diversity as Revealed by the. *Science* 307, 1576–1581. URL: <http://www.ncbi.nlm.nih.gov/pubmed/15718430>, doi:10.1126/science.1108806.
- Torson, J.M., Becker, K.J., 1997. ISIS - A Software Architecture for Processing Planetary Images. *Lpsc Xxviii* 28, 1443.
- Viviano-Beck, C.E., Seelos, F.P., Murchie, S.L., Kahn, E.G., Seelos, K.D., Taylor, H.W., Taylor, K., Ehlmann, B.L., Wisemann, S.M., Mustard, J.F., Morgan, M.F., 2014. Revised CRISM spectral parameters and summary products based on the currently detected mineral diversity on Mars. *Journal of Geophysical Research E: Planets* 119, 1403–1431. doi:10.1002/2014JE004627.